

Geophysical Research Letters

RESEARCH LETTER

10.1029/2019GL085108

Key Points:

- We have investigated the correlation between lower-band chorus waves and electron beam-like distribution using THEMIS data.
- Along with quasi-parallel chorus waves, a weak electron beam can be observed, which is caused by Landau resonance with waves.
- But for oblique chorus waves, the electron beam-like distribution should be a precondition for exciting waves rather than caused by waves.

Correspondence to:

X. Gao,
gaoxl@mail.ustc.edu.cn

Citation:

Chen, R., Gao, X., Lu, Q., & Wang, S. (2019). Unraveling the correlation between chorus wave and electron beam-like distribution in the Earth's magnetosphere. *Geophysical Research Letters*, 46, 11,671–11,678. <https://doi.org/10.1029/2019GL085108>

Received 23 AUG 2019

Accepted 24 SEP 2019

Accepted article online 15 OCT 2019

Published online 6 NOV 2019

Unraveling the Correlation Between Chorus Wave and Electron Beam-Like Distribution in the Earth's Magnetosphere

Rui Chen^{1,2} , Xinliang Gao^{1,2} , Quanming Lu^{1,2} , and Shui Wang^{1,2}

¹CAS Key Lab of Geospace Environment, School of Earth and Space Sciences, University of Science and Technology of China, Hefei, China, ²CAS Center for Excellence in Comparative Planetology, Hefei, China

Abstract In this letter, we have investigated the correlation between lower band chorus waves and electron beam-like distribution with long-term THEMIS data. Cold, hot, and beam electrons are assumed in the plasma. For quasi-parallel chorus waves, they are usually observed along with a relatively weak electron beam. Moreover, the density ratio between beam and hot electrons n_b/n_h is positively correlated with the wave parallel electric field and inversely correlated with the hot electron density, in agreement with a formation of the beam by Landau acceleration during wave propagation, while, along with oblique waves, there typically exists a strong electron beam. Notably, the n_b/n_h is found to be independent of both the parallel electric field and hot electron density, indicating that the electron beam-like distribution should be a precondition for exciting oblique waves rather than caused by waves. Our study provides some new insights into understanding the generation and evolution of chorus waves.

Plain Language Summary The interaction between whistler-mode chorus waves and electrons has long been a hot topic, which is important for understanding the evolution and generation of chorus waves. Both theoretical and simulation studies have indicated that quasi-parallel chorus waves are initially excited near the magnetic equator and then propagate toward high-latitude regions with increasing wave normal angles and enhanced parallel electric fields. During the propagation, the Landau resonance between chorus waves and electrons begins to take effect, causing the damping of waves and the formation of local electron beam. Within the equatorial region, there also exist a number of oblique chorus waves with large wave normal angles, which should be also locally excited. To generate oblique waves, a beam-like electron distribution is needed to suppress the Landau damping of oblique chorus waves, which should already exist before those waves. Although the two physical pictures are well known in this community, actually, there is still a lack of observational support. In this paper, we have made some new progress in understanding these two different scenarios by studying the correlation between chorus waves and electron beam-like distribution with long-term THEMIS data.

1. Introduction

Chorus waves are one of the most intense electromagnetic emissions in the Earth's inner magnetosphere, whose frequency typically ranges from 0.1 to $0.8f_{ce}$, where f_{ce} is the equatorial electron gyrofrequency (Burtis & Helliwell, 1969; Gao et al., 2016b; Gao et al., 2017a; Tsurutani & Smith, 1974). They have drawn much attention because of their key role in controlling electron dynamics in the Van Allen radiation belt (Ni et al., 2008; Reeves et al., 2013; Thorne et al., 2010; Thorne et al., 2013). The free energy to generate chorus waves comes from anisotropic hot (tens of keV) electrons injected from the plasma sheet during active periods (Gao et al., 2014; Li et al., 2010a; Omura et al., 2008). Based on previous theoretical and simulation studies, lower band chorus waves are generally considered to be excited near the magnetic equator with very small wave normal angles (Chen et al., 2013; Ke et al., 2017; Lu et al., 2019; Omura et al., 2008). Then, they will propagate toward high-latitude regions with increasing wave normal angles and enhanced parallel electric fields (Chen et al., 2013; Ke et al., 2017; Lu et al., 2019). As a result, the Landau resonance between chorus waves and electrons begins to take effect, causing the damping of chorus waves and parallel acceleration of electrons (Chen et al., 2013; Ke et al., 2017; Lu et al., 2019). In this scenario, a beam-like or plateau structure is expected to form in the electron parallel velocity distribution around the phase velocity of chorus wave, while, within the equatorial region, there also exist a number of oblique lower band chorus

waves with large wave normal angles (Agapitov et al., 2013; Gao et al., 2018; Li et al., 2011, 2013), which cannot be simply explained by the propagation effect. Whether these waves are generated through the cyclotron resonance or Landau resonance, a beam-like electron distribution is needed to suppress the Landau damping of chorus waves at large wave normal angles (Artemyev et al., 2016; Gao et al., 2016a; Li et al., 2016; Mourenas et al., 2015). In this case, the beam-like electron distribution should be considered as a precondition for the wave excitation rather than the feedback caused by waves. These two scenarios have been theoretically proposed and verified in selected observations (Li et al., 2016) for the second scenario and statistically (Min et al., 2014) for the first scenario. However, there is still a lack of statistical observational support for the second scenario, and no statistical comparison has ever been performed between electron distributions measured during these two different kinds of events, that is, when weakly oblique or very oblique lower band chorus waves are observed around the equator.

In this letter, we have statistically investigated the correlation between chorus waves and electron beam-like distribution by evaluating the density ratio between beam and hot electrons with nearly 7-year THEMIS data and uncovered two different scenarios for quasi-parallel and oblique chorus waves.

2. THEMIS Instruments

THEMIS mission is composed of five identical probes (THEMIS A, B, C, D, and E), which are placed in highly elliptical orbits and near the magnetic equator with apogees above $10 R_E$ and perigees below $2 R_E$ (Angelopoulos, 2008). Chorus waves are captured by the search-coil magnetometer (SCM, Le Contel et al., 2008; Roux et al., 2008) and electric field instrument (EFI, Bonnell et al., 2008), which simultaneously measure triaxial magnetic and electric fields with a sampling frequency up to ~ 8 kHz. Each waveform burst lasts about 6–8 s, while, the electron distributions are provided by the electro-static analyzer (ESA; McFadden et al., 2008), covering an energy range from a few electron volt to ~ 30 keV. Here, the total electron density is inferred from the spacecraft potential and electron thermal speed (Li et al., 2010b). And the background magnetic field used to estimate the equatorial electron gyrofrequency is measured by the fluxgate magnetometer (FGM, Auster et al., 2008). Following the procedure developed by Bortnik et al. (Bortnik et al., 2007; essentially an implementation of Means, 1972), we can obtain the polarization properties of chorus waves by analyzing three components of magnetic fields.

3. Observational Results

The chorus waves are collected from three inner probes (THEMIS A, D, and E) between $L = 5$ and 10 during the period from 1 June 2008 to 31 December 2014 based on the same criteria used in Gao et al. (2014). Two representative examples are displayed in Figure 1, including (a) the spectrogram of total magnetic fields B_t , (b) spectrogram of parallel electric fields E_{\parallel} , (c) a flag Pf , (d) wave normal angle θ , and (e) magnetic amplitude B_w . The propagating direction (Pf) of chorus waves is determined by both the direction of the Poynting flux vector and radial component of the ambient magnetic field (Gao et al., 2017b; Li et al., 2013). Here $Pf = -1$ means propagating direction toward the magnetic equator, while $Pf = 1$ means propagating direction toward the polar region. The magnetic amplitude at each time is obtained by integrating the magnetic power over $0.1-0.5f_{ce}$. As shown in Figure 1c, both chorus events are propagating away from the magnetic equator. Chorus waves in Event I are quasi-parallel ($\theta < 45^\circ$), while waves in Event II are quite oblique ($\theta > 45^\circ$; Figure 1d). Although the magnetic power of Event II is about two orders lower than that of Event I, the powers of parallel electric fields of two events are comparable (Figure 1b). In each event, the time t_s corresponding to the maximum magnetic amplitude has been chosen to extract detailed wave parameters, which has been marked by red star in Figure 1e.

The magnetic power B_t , parallel electric power E_{\parallel} , and wave normal angle θ as a function of frequency at t_s are given in Figures 2a and 2b for Events I and II, respectively. Taking Event I as an example, we first find the peak frequency f_p with the maximum magnetic power. Then, we calculate the average wave frequency f_{ave} and wave normal angle θ_{ave} weighted by the magnetic power over three adjacent frequency bins around f_p . Meanwhile, the parallel electric field amplitude $E_{\parallel w}$ is obtained by integrating over the same frequency bins. The Landau resonance between chorus wave and electron works only when the parallel velocity of electron is close to the parallel phase velocity of wave, that is, $v_{\parallel} = \omega/k\cos\theta$, where ω and k are wave angular

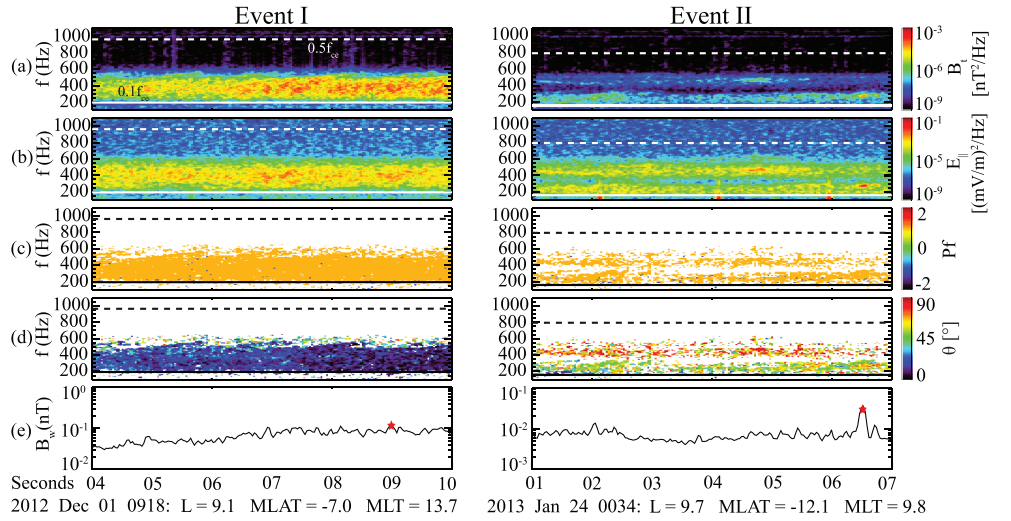


Figure 1. (a) The spectrogram of total magnetic fields B_t , (b) spectrogram of parallel electric fields E_{\parallel} , (c) a flag Pf , (d) wave normal angle θ , and (e) magnetic amplitude B_w . In all panels, the solid and dashed horizontal lines in white or black represent 0.1 and $0.5f_{ce}$, respectively.

frequency and wave number, respectively. For simplicity, the wave number is estimated by employing the dispersion relation of whistler mode in a cold plasma (Stix, 1962):

$$\left(\frac{kc}{\omega}\right)^2 = -\frac{\omega_{pe}^2}{\omega(\omega - \Omega_{ce}\cos\theta)}, \quad (1)$$

where Ω_{ce} , ω_{pe} , and c are the electron gyrofrequency, plasma frequency, and light speed, respectively. Note that the background magnetic field and density are chosen at the time closest to t_s during the calculation. Therefore, the Landau resonant velocity v_L of electron is given by $\omega/k\cos\theta$. Finally, we record these wave parameters (i.e., θ_{ave} , $E_{\parallel w}$, and v_L) for this event to further analyze the parallel velocity distribution of electrons.

The electron parallel velocity distributions (black dots) for Events I and II are shown in Figures 2c and 2d, respectively, which are obtained from ESA data at the time closest to t_s . For ESA data, there are eight pitch angle channels ranging from 11.25° to 168.75° . In this study, the 11.25° and 168.75° channels will be treated as the parallel and antiparallel directions for convenience, respectively. The Landau resonant velocity of electron has been marked by the vertical dashed line in Figure 2c or 2d. Then, we choose six adjacent data points (red circles) around the Landau resonant velocity to fit the electron parallel velocity distribution. Note that since only the parallel velocity distribution is considered in the following investigation, the precise anisotropy of the full distribution is unimportant. Accordingly, we assume that the electron distribution function $f_e = f_c + f_h + f_b$ is a combination of three distribution functions (cold, hot, and beam, respectively) with

$$f_c = n_c \left(\frac{m_e}{2\pi T_c}\right)^{\frac{3}{2}} \exp\left(-\frac{v_{\parallel}^2}{v_{tc}^2}\right), \quad (2)$$

$$f_h = n_h \left(\frac{m_e}{2\pi T_h}\right)^{\frac{3}{2}} \exp\left(-\frac{v_{\parallel}^2}{v_{th}^2}\right), \quad (3)$$

$$f_b = n_b \left(\frac{m_e}{2\pi T_b}\right)^{\frac{3}{2}} \exp\left[-\frac{(v_{\parallel} - v_L)^2}{v_{tb}^2}\right], \quad (4)$$

where n_j , T_j , and v_{ij} ($j = c, h, \text{ or } b$) are the number density, temperature, and thermal velocity of j component. It is worth noting that the bulk velocity of electron beam is fixed at the Landau resonant velocity v_L , where the interaction between chorus waves and electrons in the parallel direction is most intensive. Since the

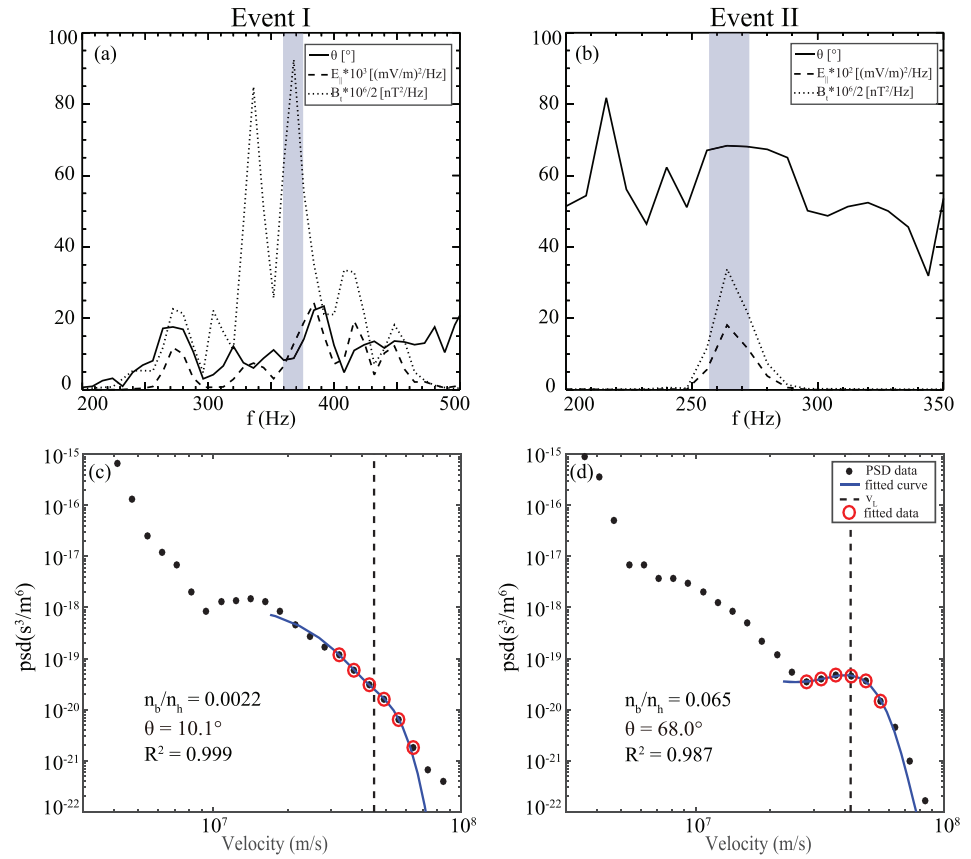


Figure 2. (a and b) The magnetic power B_t , parallel electric power E_{\parallel} , and wave normal angle θ as a function of frequency at t_s of Events I and II, respectively. In each panel, the shaded region represents the selected frequency bins to calculate mean wave parameters. (c and d) The electron parallel velocity distribution. The black dots are observed data from electrostatic analyzer (ESA) instrument, while six of them marked by red cycles are chosen to perform the fitting. The blue line is the fitted distribution function. We have also marked the Landau resonance velocity with the vertical dashed line.

temperature of cold electrons ($\sim eV$) is typically much smaller than that of hot or beam component ($\sim keV$), the parallel electron distribution around v_L approximately becomes

$$f_e \approx f_h + f_b = n_h \left(\frac{m_e}{2\pi T_h} \right)^{3/2} \exp\left(-\frac{v_{\parallel}^2}{v_{th}^2}\right) + n_b \left(\frac{m_e}{2\pi T_b} \right)^{3/2} \exp\left[-\frac{(v_{\parallel} - v_L)^2}{v_{tb}^2}\right]. \quad (5)$$

We have employed the least square method to fit the distribution curve, which is plotted as the blue line in Figure 2c or 2d. Meanwhile, we can also get the n_b , n_h , and the ratio between them n_b/n_h . Here, the parameter n_b/n_h is utilized to quantitatively describe the correlation between chorus waves and electron beam-like distribution. The high parameter R^2 , defined as $R^2 = 1 - SSE/SST$ (SSE is the sum of squares of the difference between the fitted result and the original data; SST is the sum of squares of the difference between the original data and the mean value), indicates the high reliability of calculated fitting parameters. In this study, we only retain those events in which $R^2 > 0.9$. In Event I, we can hardly tell the presence of a beam-like structure around v_L in the parallel electron distribution, since the ratio n_b/n_h is very small, that is, 0.0022. However, in Event II, it is clearly found that there is a distinct “plateau” located at v_L , suggesting that there is a significant beam component ($n_b/n_h \sim 0.065$) accompanying chorus waves.

It is worth noting that we have only focused on the lower band waves regardless of their spectral structures in this study. In this study, we have analyzed a much larger database than Min et al. (2014) and also developed a method to directly evaluate the beam-like component. We have selected about 1,060 chorus events in total. They are typically detected at the low magnetic latitudes (-20° to 20° limited by the range of latitudes

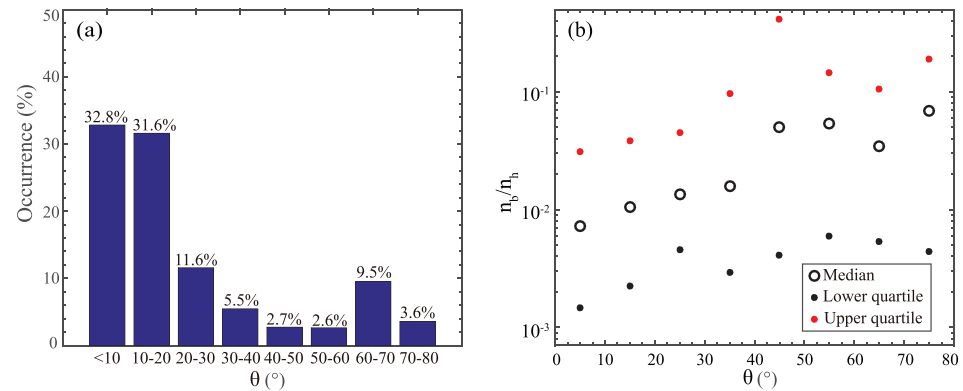


Figure 3. (a) The occurrence rate of wave normal angle for chorus waves and (b) the median density ratio n_b/n_h (black circle) in different categories of wave normal angle with the first and third quartiles marked by black and red dots, respectively.

covered by THEMIS) over all magnetic local time (Gao et al., 2014). The event inside the plasmopause or outside the magnetopause has already been excluded following the method in Li, Thorne, Nishimura, et al. (2010a). Moreover, those chorus events in which the calculated Landau resonant energy $\frac{1}{2} m_e v_L^2$ is out of the energy coverage of ESA (i.e., a few eV to 30 keV for electrons) are also removed in our study.

Figure 3a shows the occurrence rate of chorus waves as a function of the wave normal angle. The occurrence rate is defined as the ratio between the numbers of wave events in each category and total events. Just as mentioned above, chorus waves captured by THEMIS probes are not far from their main source region, that is, the magnetic equator. Therefore, they tend to have small wave normal angles ($\theta < 45^\circ$) even though the propagating effect plays a role in increasing the wave normal angle. As shown in Figure 3a, nearly 80% of chorus waves are quasi-parallel with $\theta < 45^\circ$, which is consistent with previous statistical results (Gao et al., 2014; Li et al., 2011), while there is also a significant population of chorus waves having very large wave normal angles ($\theta > 45^\circ$). These oblique chorus waves have been believed to be locally excited by hot electrons, which is supported by both theoretical and observational studies (Agapitov et al., 2016; Gao, Lu, et al., 2016a; Li et al., 2016; Mourenas et al., 2015). The correlation between chorus waves and electron beam-like distribution (i.e., n_b/n_h) as a function of the wave normal angle is displayed in Figure 3b. Overall, the n_b/n_h is generally larger than 0.01, suggesting that the majority of chorus waves is found to be with a noticeable beam-like component of electrons. In fact, there is only a weak trend that the n_b/n_h increases with the increase of the wave normal angle. Instead, there is a remarkable difference between quasi-parallel ($\theta < 45^\circ$) and oblique ($\theta > 45^\circ$) chorus waves. The median values of n_b/n_h for oblique waves are at least five times as large as those for quasi-parallel waves. In other words, the oblique chorus wave is usually accompanied by a more significant electron beam.

Therefore, we divide chorus events into two categories, that is, quasi-parallel ($\theta < 45^\circ$) and oblique ($\theta > 45^\circ$) events, and further investigate the dependences of n_b/n_h on the parallel electric field amplitude E_{\parallel} and hot electron density n_h . To remove the effects of various background magnetic field B_0 and plasma density n_0 , we have normalized E_{\parallel} and n_h by $B_0 V_{Ae}$ (V_{Ae} is given by $B_0 / \sqrt{\mu_0 n_0 m_e}$) and n_0 , respectively. Figures 4a and 4b present the scatter plots of chorus events in the $(E_{\parallel}/B_0 V_{Ae}, n_h/n_0)$ plane with color-coded n_b/n_h . For clarity, we have also shown the median n_b/n_h in the $(E_{\parallel}/B_0 V_{Ae}, n_h/n_0)$ plane in Figures 4c and 4d. For quasi-parallel chorus waves, the majority of them is accompanied by a relatively weak electron beam with n_b/n_h around 0.01. The density n_b of electrons accelerated by E_{\parallel} near $v_{\parallel} = v_L$ should depend on E_{\parallel} and on the initial $f_h(v_L)$. For $\theta < 45^\circ$ events, n_b/n_h is small, and v_L is on the fast-decreasing shoulder of the distribution. Then, the density n_h of f_h fitted around v_L depends (exponentially) strongly on the varying v_{th} but only weakly (linearly) on $f_h(v_L)$. As a result, n_h should be statistically mostly independent of $f_h(v_L)$ and n_b , and n_b/n_h is expected to decrease as n_h increases. Therefore, the density ratio n_b/n_h is positively correlated with the parallel electric field amplitude $E_{\parallel}/B_0 V_{Ae}$ but inversely correlated with hot electron density n_h/n_0 . As shown in Figure 4c, from bottom right to up left, the median density ratio n_b/n_h gradually increases up to comparable to 1 from $\sim 10^{-3}$. This result well supports the physical picture that the electron beam-like distribution is

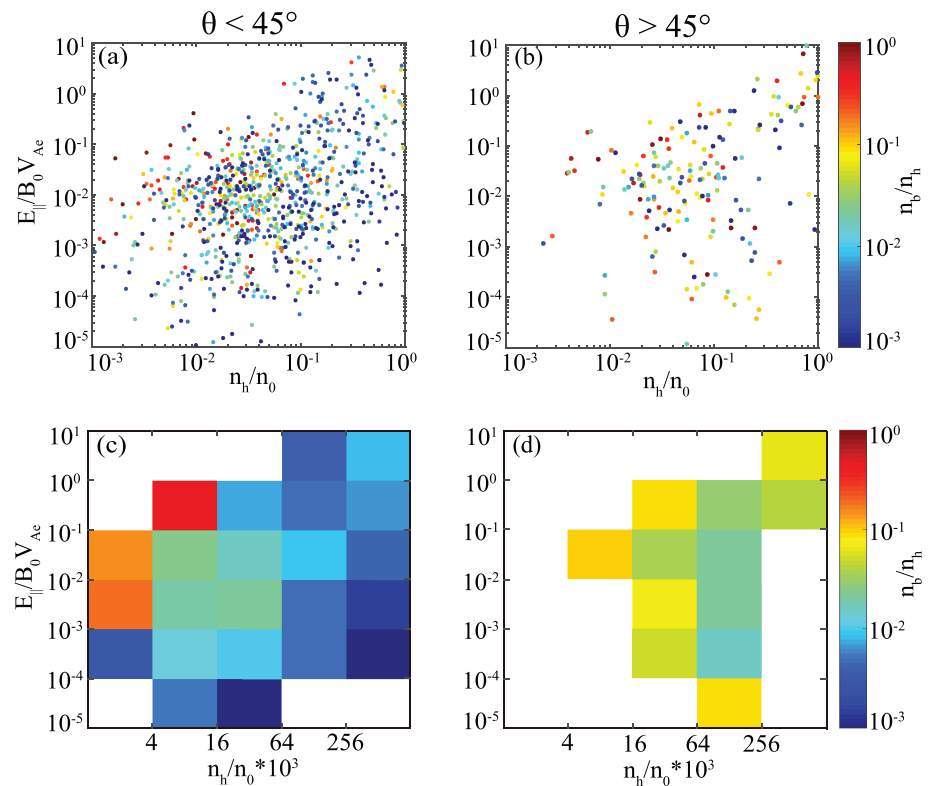


Figure 4. (a and b) The scatter plots of chorus events in the $(E_{\parallel}/B_0V_{Ae}, n_h/n_0)$ plane with color-coded n_b/n_h for two categories (i.e., $\theta < 45^\circ$ and $\theta > 45^\circ$) and (c and d) the median value of n_b/n_h in the $(E_{\parallel}/B_0V_{Ae}, n_h/n_0)$ plane. In panels c and d, we only retain those bins with more than three wave events.

caused by the Landau resonance during the propagation of chorus waves. However, for oblique chorus waves, they tend to be observed with a strong electron beam with n_b/n_h around 0.05. Unlike the case of quasi-parallel waves, the median density ratio n_b/n_h is independent of either E_{\parallel}/B_0V_{Ae} or n_h/n_0 (Figure 4d), suggesting that the electron beam-like distribution is more like a necessary condition for the generation of oblique waves rather than caused by waves.

4. Summary and Discussion

In this letter, we have studied the correlation between lower band chorus waves and electron beam-like distribution by evaluating the density ratio between beam and hot electrons n_b/n_h with nearly 7-year THEMIS data. The larger n_b/n_h indicates a more significant electron beam-like or plateau structure located around the Landau resonant velocity in the parallel velocity distribution. Two different scenarios have been uncovered. Quasi-parallel chorus waves are usually observed along with a relatively weak electron beam with n_b/n_h typically smaller than 0.02. Moreover, the n_b/n_h is positively correlated with the parallel electric field amplitude E_{\parallel}/B_0V_{Ae} and inversely correlated with hot electron density n_h/n_0 . This result indicates that the electron beam-like (or plateau) distribution is caused by Landau resonance during wave propagation. In contrast, oblique chorus waves are accompanied by a strong electron beam with n_b/n_h larger than 0.04. In particular, the n_b/n_h is found to be independent of both E_{\parallel}/B_0V_{Ae} and n_h/n_0 , suggesting that the electron beam-like distribution is more like a precondition for exciting oblique waves rather than caused by waves.

Chorus waves are commonly believed to be excited by anisotropic hot electrons at the magnetic equator, whose wave normal angles are typically very small (Chen et al., 2013; Ke et al., 2017; Lu et al., 2019; Omura et al., 2008). Then, they will propagate toward high-latitude regions with increasing wave normal angles (Chen et al., 2013; Ke et al., 2017; Lu et al., 2019). Meanwhile, the parallel electric field of chorus waves also becomes significant, which will accelerate electrons in the parallel direction through the

Landau resonance (Agapitov et al., 2015, 2016; Artemyev et al., 2016; Min et al., 2014). Therefore, a beam-like or plateau structure is expected to form in the electron parallel velocity distribution around the phase velocity of chorus wave, which is consistent with the results of previous work (Agapitov et al., 2015, 2016; Artemyev et al., 2016; Min et al., 2014). Min et al. (2014) provided evidence for the Landau resonant interactions between electrons and chorus waves with 4-year THEMIS data. It is readily accepted that the stronger parallel electric field and lower hot electron density will result in the larger n_b/n_h or more significant beam-like or plateau structure. This trend can be clearly observed in Figure 4c, which provides a strong evidence to support the above physical picture of wave evolution. On the other hand, there is also a population of oblique chorus waves with large wave normal angles (Gao et al., 2018; Li et al., 2011), which cannot be simply explained by the propagation effect. Both theoretical and observational studies have pointed out that these waves can be locally excited but a beam-like electron distribution is required to suppress the Landau damping of oblique chorus waves (Artemyev et al., 2016; Gao, Lu, et al., 2016a; Li et al., 2016; Mourenas et al., 2015). In this case, the beam-like electron distribution already exists before the excitation of chorus waves. Then, we can understand why the n_b/n_h is independent of the wave fields but remains at a high level for oblique waves. Our study provides some new observational clues for understanding the generation and evolution of chorus waves in the Earth's magnetosphere.

Acknowledgments

This work was supported by the NSFC (Grant 41631071, 41527804, 41774151, and 41774169), Key Research Program of Frontier Sciences CAS (QYZDJ-SSW-DQC010), Youth Innovation Promotion Association of Chinese Academy of Sciences (2016395), and Young Elite Scientists Sponsorship Program by CAST (2018QNR001). We also acknowledge the entire THEMIS instrument group and the THEMIS data obtained from <http://themis.ssl.berkeley.edu/data/themis> website.

References

- Agapitov, O., Artemyev, A., Krasnoselskikh, V., Khotyaintsev, Y. V., Mourenas, D., Breuillard, H., et al. (2013). Statistics of whistler-mode waves in the outer radiation belt: Cluster STAFF-SA measurements. *Journal of Geophysical Research: Space Physics*, *118*, 3407–3420. <https://doi.org/10.1002/jgra.50312>
- Agapitov, O. V., Artemyev, A. V., Mourenas, D., Mozer, F. S., & Krasnoselskikh, V. (2015). Nonlinear local parallel acceleration of electrons through Landau trapping by oblique whistler mode waves in the outer radiation belt. *Geophysical Research Letters*, *42*, 10,140–10,149. <https://doi.org/10.1002/2015GL066887>
- Agapitov, O. V., Mourenas, D., Artemyev, A. V., & Mozer, F. S. (2016). Exclusion principle for very oblique and parallel lower band chorus waves. *Geophysical Research Letters*, *43*, 11,112–11,120. <https://doi.org/10.1002/2016GL071250>
- Angelopoulos, V. (2008). The THEMIS mission. *Space Science Reviews*, *141*(1–4), 5–34. <https://doi.org/10.1007/s11214-008-9336-1>
- Artemyev, A., Agapitov, O., Mourenas, D., Krasnoselskikh, V., Shastun, V., & Mozer, F. (2016). Oblique whistler-mode waves in the Earth's inner magnetosphere: Energy distribution, origins, and role in radiation belt dynamics. *Space Science Reviews*, *200*, 261–355. <https://doi.org/10.1007/s11214-016-0252-5>
- Auster, H. U., Glassmeier, K. H., Magnes, W., Aydogar, O., Baumjohann, W., Constantinescu, D., et al. (2008). The THEMIS fluxgate magnetometer. *Space Science Reviews*, *141*(1–4), 235–264. <https://doi.org/10.1007/s11214-008-9365-9>
- Bonnell, J. W., Mozer, F. S., Delory, G. T., Hull, A. J., Ergun, R. E., Cully, C. M., et al. (2008). The electric field instrument (EFI) for THEMIS. *Space Science Reviews*, *141*, 303–341. <https://doi.org/10.1007/s11214-008-9469-2>
- Bortnik, J., Cutler, J. W., Dunson, C., & Bleier, T. E. (2007). An automatic wave detection algorithm applied to Pc1 pulsations. *Journal of Geophysical Research*, *112*, A04204. <https://doi.org/10.1029/2006JA011900>
- Burtis, W. J., & Helliwell, R. A. (1969). Banded chorus—A new type of VLF radiation observed in the magnetosphere by OGO 1 and OGO 3. *Journal of Geophysical Research*, *74*, 3002–3010. <https://doi.org/10.1029/JA074i011p03002>
- Chen, L., Thorne, R. M., Li, W., & Bortnik, J. (2013). Modeling the wave normal distribution of chorus waves. *Journal of Geophysical Research: Space Physics*, *118*, 1074–1088. <https://doi.org/10.1029/2012JA018343>
- Gao, X., Ke, Y., Lu, Q., Chen, L., & Wang, S. (2017a). Generation of multiband chorus in the Earth's magnetosphere: 1-D PIC simulation. *Geophysical Research Letters*, *44*, 618–624. <https://doi.org/10.1002/2016GL072251>
- Gao, X., Lu, Q., & Wang, S. (2017b). First report of resonant interactions between whistler mode waves in the Earth's magnetosphere. *Geophysical Research Letters*, *44*, 5269–5275. <https://doi.org/10.1002/2017GL073829>
- Gao, X., Lu, Q., & Wang, S. (2018). Statistical results of multiband chorus by using THEMIS waveform data. *Journal of Geophysical Research: Space Physics*, *123*, 5506–5515. <https://doi.org/10.1029/2018JA025393>
- Gao, X. L., Li, W., Thorne, R. M., Bortnik, J., Angelopoulos, V., Lu, Q. M., et al. (2014). New evidence for generation mechanisms of discrete and hiss-like whistler mode waves. *Geophysical Research Letters*, *41*, 4905–4811. <https://doi.org/10.1002/2014GL060707>
- Gao, X. L., Lu, Q. M., Bortnik, J., Li, W., Chen, L., & Wang, S. (2016a). Generation of multiband chorus by lower band cascade in the Earth's magnetosphere. *Geophysical Research Letters*, *43*, 2343–2350. <https://doi.org/10.1002/2016GL068313>
- Gao, X. L., Mourenas, D., Li, W., Artemyev, A. V., Lu, Q. M., Tao, X., & Wang, S. (2016b). Observational evidence of generation mechanisms for very oblique lower band chorus using THEMIS waveform data. *Journal of Geophysical Research: Space Physics*, *121*, 6732–6748. <https://doi.org/10.1002/2016JA022915>
- Ke, Y., Gao, X., Lu, Q., Wang, X., & Wang, S. (2017). Generation of rising-tone chorus in a two-dimensional mirror field by using the general curvilinear PIC code. *Journal of Geophysical Research: Space Physics*, *122*, 8154–8165. <https://doi.org/10.1002/2017JA024178>
- Le Contel, O., Roux, A., Robert, P., Coillot, C., Bouabdellah, A., de laPorte, B., et al. (2008). First results of the THEMIS search coil magnetometers. *Space Science Reviews*, *141*(1–4), 509–534. <https://doi.org/10.1007/s11214-008-9371-y>
- Li, W., Thorne, R. M., Nishimura, Y., Bortnik, J., Angelopoulos, V., McFadden, J. P., et al. (2010a). THEMIS analysis of observed equatorial electron distributions responsible for the chorus excitation. *Journal of Geophysical Research*, *115*, A00F11. <https://doi.org/10.1029/2009JA014845>
- Li, W., Bortnik, J., Thorne, R. M., & Angelopoulos, V. (2011). Global distribution of wave amplitudes and wave normal angles of chorus waves using THEMIS wave observations. *Journal of Geophysical Research*, *116*, A12205. <https://doi.org/10.1029/2011JA017035>
- Li, W., Bortnik, J., Thorne, R. M., Cully, C. M., Chen, L., Angelopoulos, V., et al. (2013). Characteristics of the Poynting flux and wave normal vectors of whistler-mode waves observed on THEMIS. *Journal of Geophysical Research: Space Physics*, *118*, 1461–1471. <https://doi.org/10.1002/jgra.50176>

- Li, W., Thorne, R. M., Bortnik, J., Nishimura, Y., Angelopoulos, V., Chen, L., et al. (2010b). Global distributions of suprathermal electrons observed on THEMIS and potential mechanisms for access into the plasmasphere. *Journal of Geophysical Research*, *115*, A00J10. <https://doi.org/10.1029/2010JA015687>
- Li, W., Mourenas, D., Artemyev, A. V., Bortnik, J., Thorne, R. M., Kletzing, C. A., et al. (2016). Unraveling the excitation mechanisms of highly oblique lower band chorus waves. *Geophysical Research Letters*, *43*, 8867–8875. <https://doi.org/10.1002/2016GL070386>
- Lu, Q., Ke, Y., Wang, X., Liu, K., Gao, X., Chen, L., & Wang, S. (2019). Two-dimensional general curvilinear particle-in-cell (gcPIC) simulation of rising-tone chorus waves in a dipole magnetic field. *Journal of Geophysical Research: Space Physics*, *124*, 4157–4167. <https://doi.org/10.1029/2019JA026586>
- McFadden, J. P., Carlson, C. W., Larson, D., Ludlam, M., Abiad, R., Elliott, B., et al. (2008). The THEMIS ESA plasma instrument and in-flight calibration. *Space Science Reviews*, *141*(1–4), 277–302. <https://doi.org/10.1007/s11214-008-9440-2>
- Means, J. D. (1972). Use of 3-dimensional covariance matrix in analyzing polarization properties of plane waves. *Journal of Geophysical Research*, *77*(28), 5551–5559. <https://doi.org/10.1029/JA077i028p05551>
- Min, K., Liu, K., & Li, W. (2014). Signatures of electron Landau resonant interactions with chorus waves from THEMIS observations. *Journal of Geophysical Research: Space Physics*, *119*, 5551–5560. <https://doi.org/10.1002/2014JA019903>
- Mourenas, D., Artemyev, A. V., Agapitov, O. V., Krasnoselskikh, V., & Mozer, F. S. (2015). Very oblique whistler generation by low-energy electron streams. *Journal of Geophysical Research: Space Physics*, *120*, 3665–3683. <https://doi.org/10.1002/2015JA021135>
- Ni, B., Thorne, R. M., Shprits, Y. Y., & Bortnik, J. (2008). Resonant scattering of plasma sheet electrons by whistler-mode chorus: Contribution to diffuse auroral precipitation. *Geophysical Research Letters*, *35*, L11106. <https://doi.org/10.1029/2008GL034032>
- Omura, Y., Katoh, Y., & Summers, D. (2008). Theory and simulation of the generation of whistler-mode chorus. *Journal of Geophysical Research*, *113*, A04223. <https://doi.org/10.1029/2007JA012622>
- Reeves, G. D., Spence, H. E., Henderson, M. G., Morley, S. K., Friedel, R. H. W., Funsten, H. O., et al. (2013). Electron acceleration in the heart of the Van Allen radiation belts. *Science*, *341*(6149), 991–994. <https://doi.org/10.1126/science.1237743>
- Roux, A., Le Contel, O., Coillot, C., Bouabdellah, A., de la Porte, B., Alison, D., et al. (2008). The search coil magnetometer for THEMIS. *Space Science Reviews*, *141*(1–4), 265–275. <https://doi.org/10.1007/s11214-008-9455-8>
- Stix, T. H. (1962). *The theory of plasma waves*. New York: McGraw-Hill.
- Thorne, R. M., Li, W., Ni, B., Ma, Q., Bortnik, J., Chen, L., et al. (2013). Rapid local acceleration of relativistic radiation-belt electrons by magnetospheric chorus. *Nature*, *504*(7480), 411–414. <https://doi.org/10.1038/nature12889>
- Thorne, R. M., Ni, B., Tao, X., Horne, R. B., & Meredith, N. P. (2010). Scattering by chorus waves as the dominant cause of diffuse auroral precipitation. *Nature*, *467*(7318), 943–946. <https://doi.org/10.1038/nature09467>
- Tsurutani, B. T., & Smith, E. J. (1974). Postmidnight chorus: A substorm phenomenon. *Journal of Geophysical Research*, *79*, 118–127. <https://doi.org/10.1029/JA079i001p00118>